**MASTER COPY**: PLEASE KEEP THIS "MEMORANDUM OF TRANSMITTAL" BLANK FOR REPRODUCTION PURPOSES. WHEN REPORTS ARE GENERATED UNDER THE ARO SPONSORSHIP, FORWARD A COMPLETED COPY OF THIS FORM WITH EACH REPORT SHIPMENT TO THE ARO. THIS WILL ASSURE PROPER IDENTIFICATION. NOT TO BE USED FOR INTERIM PROGRESS REPORTS; SEE PAGE 2 FOR INTERIM PROGRESS REPORT INSTRUCTIONS.

## MEMORANDUM OF TRANSMITTAL

U.S. Army Research Office
ATTN: AMSRL-RO-BI (TR)
P.O. Box 12211
Research Triangle Park, NC 27709-2211

☐ Reprint (Orig + 2 copies)
☐ Technical Report (Orig + 2 copies)
☑ Manuscript (1 copy)
☐ Final Progress Report (Orig + 2 copies)
☐ Related Materials, Abstracts, Theses (1 copy)

CONTRACT/GRANT NUMBER: W911NF0410224 (46637CIMUR)

REPORT TITLE: Channel Diversity in Random Wireless Networks

is forwarded for your information.

Accepted in:
IEEE Transactions on Wireless Communications

Sincerely,

Dr. James Zeidler
Department of Electrical and Computer Engineering
University of California, San Diego

# REPORT DOCUMENTATION PAGE

Form Approved
OMB NO. 0704-0188



| 1. AGENCY USE ONLY ( Leave Blank) | 2. REPORT DATE | 3. REPORT TYPE AND DATES COVERED |
|---|---|---|
| | 2009 | Manuscript 2009 |

4. TITLE AND SUBTITLE
Channel Diversity in Random Wireless Networks

5. FUNDING NUMBERS
W911NF0410224

6. AUTHOR(S)
Kostas Stamatiou, John G. Proakis, and James R. Zeidler

7. PERFORMING ORGANIZATION NAME(S) AND ADDRESS(ES)
University of California - San Diego
9500 Gilman Drive, Mail Code 0407 La Jolla, CA 92093-0407

8. PERFORMING ORGANIZATION REPORT NUMBER
N/A

9. SPONSORING / MONITORING AGENCY NAME(S) AND ADDRESS(ES)
U. S. Army Research Office
P.O. Box 12211
Research Triangle Park, NC 27709-2211

10. SPONSORING / MONITORING AGENCY REPORT NUMBER
46637CIMUR

11. SUPPLEMENTARY NOTES
The views, opinions and/or findings contained in this report are those of the author(s) and should not be construed as an official Department of the Army position, policy or decision, unless so designated by other documentation.

12 a. DISTRIBUTION / AVAILABILITY STATEMENT
Approved for public release; distribution unlimited

12 b. DISTRIBUTION CODE
N/A

13. ABSTRACT (Maximum 200 words)

Abstract—The goal of this paper is to explore the benefits of channel diversity in wireless ad hoc networks. Our model is that of a Poisson point process of transmitters, each with a receiver at a given distance. A packet is divided in blocks which are transmitted over different sub bands determined by random frequency hopping. At the receiver, a maximum-likelihood decoder is employed to estimate the transmitted packet/codeword. We show that, if L is the Hamming distance of the error correction code and ε is a constraint on the packet error probability, the transmission capacity of the network is proportional to $\epsilon^{1/L}$, when $\varepsilon \to 0$. The proportionality constant depends on the code selection, the packet length, the geometry of the symbol constellation and the number of receive antennas. This result implies that, at the cost of a moderate decoding complexity, large gains can be achieved by a simple interference randomization scheme during packet transmission. We also address practical issues such as channel estimation and power control. We find that reliable channel information can be obtained at the receiver without significant rate loss and demonstrate that channel inversion power control can increase the transmission capacity.

| 14. SUBJECT TERMS | 15. NUMBER OF PAGES |
|---|---|
| Frequency hopping, interference diversity, bitinterleaved coded modulation (BICM), Poisson point process | 10 |
| | 16. PRICE CODE: N/A |

| 17. SECURITY CLASSIFICATION OR REPORT | 18. SECURITY CLASSIFICATION ON THIS PAGE | 19. SECURITY CLASSIFICATION OF ABSTRACT | 20. LIMITATION OF ABSTRACT |
|---|---|---|---|
| **UNCLASSIFIED** | **UNCLASSIFIED** | **UNCLASSIFIED** | **U** |

NSN 7540-01-280-5500

**Standard Form 298 (Rev.2-89)**
Prescribed by ANSI Std. 239-18
298-102

Enclosure 1

# Channel Diversity in Random Wireless Networks

Kostas Stamatiou, *Member, IEEE,* John G. Proakis, *Life Fellow, IEEE,* and James R. Zeidler, *Fellow, IEEE*

***Abstract*—The goal of this paper is to explore the benefits of channel diversity in wireless ad hoc networks. Our model is that of a Poisson point process of transmitters, each with a receiver at a given distance. A packet is divided in blocks which are transmitted over different subbands determined by random frequency hopping. At the receiver, a maximum-likelihood decoder is employed to estimate the transmitted packet/codeword. We show that, if $L$ is the Hamming distance of the error correction code and $\epsilon$ is a constraint on the packet error probability, the transmission capacity of the network is proportional to $\epsilon^{1/L}$, when $\epsilon \to 0$. The proportionality constant depends on the code selection, the packet length, the geometry of the symbol constellation and the number of receive antennas. This result implies that, at the cost of a moderate decoding complexity, large gains can be achieved by a simple interference randomization scheme during packet transmission. We also address practical issues such as channel estimation and power control. We find that reliable channel information can be obtained at the receiver without significant rate loss and demonstrate that channel-inversion power control can increase the transmission capacity.**

***Index Terms*—Frequency hopping, interference diversity, bit-interleaved coded modulation (BICM), Poisson point process**

## I. Introduction

The study of random wireless networks has recently gathered a lot of attention in the research community [1]. The main theme of this work is the use of tools from stochastic geometry in order to characterize the performance of an ensemble of networks, for different physical, medium access control and network layer strategies. A central modeling assumption is that the network consists of a Poisson point process of transmitters, and each transmitter (TX) has a corresponding receiver (RX) at a given distance. A popular metric that quantifies the network performance is the transmission capacity, defined as the maximum spatial density of transmissions, multiplied by their rate, such that a constraint on the packet error rate is satisfied [2].

In the majority of existing papers (see overview in [1]), interference from concurrent transmissions is considered as noise and an outage probability approach is taken to model packet successes: Given the TX locations and the channels between the TXs and the reference RX, which are assumed to be constant during the transmission of a packet, a packet is successfully received if the signal-to-interference-ratio (SIR) is larger than a certain threshold. In information-theoretical terms, assuming the TXs are sending symbols from a Gaussian alphabet, a packet reception occurs when the channel mutual information is at least equal to the desired information rate [3].

In this paper, as in [4], we take an alternative approach and explore the impact of channel randomization *within* the transmission of a packet. Our motivation stems from the well known fact that channel diversity can be exploited through error correction coding in order to yield performance gains. Specifically, we consider a physical-layer scheme based on random frequency hopping (FH), bit-interleaved coded modulation (BICM) [5], and maximal ratio combining (MRC) to exploit spatial diversity at the RX. FH is preferred over Direct Sequence (DS) Spread Spectrum (SS) as the multiple-access (MA) scheme primarily because DS-SS suffers from the near-far problem in the decentralized environment of an ad hoc network [6]. Moreover, it is known that FH combined with coding exploits frequency diversity, if the hopping distance is larger than the coherence bandwidth of the channel fading, and interference diversity, as the set of interfering TXs over each dwell is potentially different. FH also simplifies the MA protocol, as no coordination is required between different TX-RX links. Regarding the choice of coding and modulation strategy, BICM is spectrally efficient and well suited for fading and interference channels, as the diversity order is determined by the Hamming distance of the employed convolutional code [5]. Finally, MRC only requires channel state information at the RX, which is desirable given that the transmission subband changes frequently across time.

We analyze the performance of the aforementioned scheme in terms of the codeword/packet error probability and evaluate the transmission capacity. Since an averaging over different channel states takes place within a packet, the information rate of the typical TX-RX link is upper-bounded by the ergodic capacity for which we provide tight upper and lower bounds. We also address practical physical-layer issues such as channel estimation, power control (PC) and channel correlation, and assess their effect on the performance via simulation.

### A. Related work

Several papers have dealt with the performance analysis of coded FH systems under MA interference, as well as partial-band interference (see, e.g., [7], [8] and Chapter 12 of [9]). A common feature of such systems is that the performance can be dramatically improved if the decoder is aware of the interference levels across the codeword. If a Reed-Solomon (RS) code is employed, the decoder declares an erasure when a symbol has been "hit"; in the case of soft-decoding, the metrics in the Viterbi decoder are weighted by the respective SIRs. In [10], RS coding combined with FSK modulation is considered in a Poisson field of interferers and the impact of the code rate on the information efficiency, i.e., the

Manuscript created June 3, 2009; revised January 24, 2010; accepted May 8, 2010. The associate editor coordinating the review of this paper and approving it for publication was M. Uysal. This work was supported by the MURI Grant W911NF-04-1-0224.

K. Stamatiou is with the University of Notre Dame, Notre Dame, IN 46556. J. G. Proakis and J. R. Zeidler are with the University of California San Diego, La Jolla, CA 92037.

product (packet success probability) $\times$ (transmission distance) $\times$ (rate), is explored. More recently, [11] has extended the work in [10] to accommodate differential unitary space-time modulation and unknown fast time-varying channels.

The use of spread-spectrum (SS) communication for ad hoc networks is discussed in [6]. The authors make an argument against interference averaging which they define as "... using DS-SS or fast FH[1] to proportionally reduce the interference level" and advocate hopping at the packet level, or interference avoidance (IA), as the preferable MA scheme for ad hoc networks. While the near-far problem of DS-SS in a decentralized environment is clear, it is not obvious why slow FH might be preferable to fast FH, apart from the fact that slow FH potentially induces less overhead in terms of code acquisition and synchronization.

### B. Contributions

This paper demonstrates that considerable gains in terms of network capacity are possible by combining FH during packet transmission and error correction coding of modest complexity. If $L$ is the Hamming distance of the convolutional code employed at the TX, $\lambda$ is the density of TXs and $M$ is the number of subbands, we show that, as $\lambda/M \to 0$, the codeword error probability follows the power law $\eta(\frac{\lambda}{M})^L$, $\eta > 0$. This leads to the conclusion that, for $\epsilon \to 0$, where $\epsilon$ is the constraint placed on the codeword error probability, the transmission capacity is proportional to $\epsilon^{1/L}$. The proportionality constant depends on the selected code, the codeword length, the geometry of the symbol constellation, as well as the term $N^{2/b}$, where $N$ is the number of RX antennas and $b > 2$ is the propagation exponent. We also derive upper and lower bounds on the ergodic capacity $C$ of the typical TX-RX link. Specifically, we show that $C > \frac{b}{2}\log_2\left(\mu N^{2/b}\frac{M}{\lambda}\right)$, where $\mu > 0$ is an appropriately defined constant.

Practical physical-layer issues are discussed such as channel estimation, PC and channel correlation. We demonstrate via simulation that, with an acceptable rate loss due to the transmission of pilot symbols, the channel fading and the interference power can be accurately estimated for decoding. With respect to PC, it is shown that channel inversion can actually enhance the capacity, since the error correction code protects the RX from the deep fades of its nearby interferers. Finally, the impact of the channel correlation is assessed as the number of subbands and/or the number of dwells is decreased and it is shown that the gains compared to slow FH are still significant.

### C. Paper organization and notation

The rest of the paper is organized as follows. Section II introduces our system model in detail. In Section III we derive the statistics of the SIR and determine the performance of the decoder under perfect CSI. The transmission capacity is defined and evaluated in Section IV. Section V discusses practical physical-layer considerations and Section VI presents our numerical results. Section VII concludes the paper.

[1]Fast FH refers to hopping on the order of a symbol or a few symbols, while slow FH, or interference avoidance, refers to hopping at the packet level.

TABLE I
COMMONLY USED SYMBOLS

| Symbol | Meaning |
|---|---|
| $R$ | Distance of typical TX-RX link |
| $\lambda$ | Density of TXs |
| $M$ | Number of subbands |
| $N$ | Number of RX antennas |
| $b$ | Path-loss exponent ($b > 2$) |
| $\alpha = 2/b$ | Stability exponent |
| $L_{\rm b}$ | Number of information bits per packet |
| $M_c$ | Number of bits per constellation symbol |
| $R_c$ | Rate of convolutional code |
| $T_d$ | Number of data symbols per dwell |
| $T_p$ | Number of pilot symbols per dwell |
| $D$ | Number of dwells |
| $L$ | Hamming distance of convolutional code |
| $P_l$ | Probability of length-$l$ error event |
| $w_l$ | Number of length-$l$ error events |
| $P_e$ | Probability of packet error |
| $C$ | Ergodic capacity of typical TX-RX link |
| $\tau_\epsilon$ | Transmission capacity under constraint $P_e = \epsilon$ |

A real (circularly symmetric complex) Gaussian random variable (r.v.) $x$ with mean 0 and variance $\sigma^2$ is denoted as $x \sim \mathcal{N}(0,\sigma^2)$ ($x \sim \mathcal{CN}(0,\sigma^2)$). A central chi-square r.v. $x$ with parameter $1/2$ and $n$ degrees of freedom is denoted as $x \sim \chi^2_n$. $\mathbf{I}_n$ is the $n \times n$ identity matrix. $(\cdot)^{\rm T}$ and $(\cdot)^{\rm H}$ denote the transpose and conjugate transpose operations, respectively. $[\mathbf{X}]_{n,t}$ denotes the $(n,t)$ element of matrix $\mathbf{X}$ and $[\boldsymbol{x}]_n$ denotes the $n^{\rm th}$ element of vector $\boldsymbol{x}$. The symbol "$\simeq$" is employed to denote asymptotic equality of two functions. A list of symbols commonly used throughout the paper is provided in Table I.

## II. System model

### A. General

We consider a network of TXs, each with a RX at a fixed distance $R$ and random orientation. The locations of the TXs are determined according to a homogeneous Poisson point process $\Pi = \{z_i\} \subset \mathbb{R}^2$, $i \in \mathbb{N}$, of density $\lambda$. The TXs send packets to their corresponding receivers concurrently and in a synchronized manner. Typically, the locations of the nodes are constant for at least the duration of a packet.

The bandwidth is divided into $M$ subbands. The channel between a typical TX-RX pair over a subband comprises flat Rayleigh fading and path loss according to the law $r^{-b}$, where $b > 2$ is the propagation exponent[2]. We assume that the coherence bandwidth of the fading is equal to the width of a subband, while the coherence time is at least equal to the duration of a *dwell*, which will be defined shortly. We also consider an interference-limited scenario, i.e., the TX power is sufficiently large that additive noise at the RX can be ignored. Initially, we assume that the TX power is the same for all TXs. Issues of PC to compensate for long-term fading, e.g., shadowing, are discussed in Section V.

Assume that a packet corresponds to $L_{\rm b}$ binary information bits, $b_1, \ldots, b_{L_{\rm b}}$, which are the input to a convolutional

[2]The constraint $b > 2$ is required in order for the interference power to be finite [1], [12].

encoder of rate $R_c < 1$[3]. The bits $c_1, \ldots, c_{k'}, \ldots, c_{L_\mathrm{b}/R_c}$ of the output codeword are interleaved and Gray-mapped to symbols $x_1, \ldots, x_k, \ldots, x_{L_\mathrm{b}/(R_c M_c)}$ from a complex PSK or QAM constellation $\mathcal{X}$ of size $|\mathcal{X}| = 2^{M_c}$, zero mean and unit average power. We assume that the one-to-one interleaver mapping $k' \leftrightarrow (k, j_{k'})$, where $j_{k'} = 1, \ldots, M_c$ is the position of $c_{k'}$ in the symbol $x_k$, is known at the RX. Next in the TX chain, the symbol sequence is divided in $D = L_\mathrm{b}/(R_c M_c T_d)$ groups[4] of size $T_d$ and each group is transmitted in a dwell, over a subband which is randomly[5] selected with probability $1/M$. If we denote the data symbols of the $d^{\mathrm{th}}$ dwell, $d = 1, \ldots, D$, as $\boldsymbol{x}_d^{\mathrm{T}}$, the sequence $\{\boldsymbol{x}_d^{\mathrm{T}}\}_{d=1}^{D}$ constitutes a packet. For convenience, we assume all transmissions are synchronized at the dwell level (the issue of asynchronous transmissions is discussed in Section V).

Consider the typical TX, located at $z_0$, and its corresponding RX, both specified by index 0, i.e., $\mathrm{TX}_0$ and $\mathrm{RX}_0$. If $\mathrm{RX}_0$ is equipped with an antenna array of size $N \geq 1$, the received data matrix in dwell $d$ is[6]

$$\mathbf{Y}_{d,0} = \boldsymbol{h}_{d,0}\boldsymbol{x}_{d,0}^{\mathrm{T}} + R^{b/2}\sum_{i\neq 0} e_{d,i} r_i^{-b/2} \mathrm{e}^{\mathrm{i}\phi_i} \boldsymbol{h}_{d,i}\boldsymbol{x}_{d,i}^{\mathrm{T}}, \qquad (1)$$

where $\boldsymbol{h}_{d,0} \sim \mathcal{CN}(\mathbf{0}, \mathbf{I}_N)$ is the fading vector between $\mathrm{TX}_0$ and $\mathrm{RX}_0$; $e_{d,i}$ is the indicator of the event that the TX located at $z_i$ (denoted as $\mathrm{TX}_i$) and at distance $r_i$ from $\mathrm{RX}_0$, occupies the same subband as $\mathrm{TX}_0$ in dwell $d$, i.e., $\mathbb{P}(e_{d,i} = 1) = 1/M$ and $\mathbb{P}(e_{d,i} = 0) = 1 - 1/M$; $\boldsymbol{h}_{d,i} \sim \mathcal{CN}(\mathbf{0}, \mathbf{I}_N)$ is the fading vector between $\mathrm{TX}_i$ and $\mathrm{RX}_0$; $\boldsymbol{x}_{d,i}^{\mathrm{T}}$ is the group of data symbols transmitted by $\mathrm{TX}_i$ in dwell $d$; and $\phi_i$ is a random phase, uniformly distributed in $[0, 2\pi)$, which models the phase offset between the $\mathrm{RX}_0$ and $\mathrm{TX}_i$. Note that the subscript $d$ in the fading vectors indicates that, in general, depending on the coherence time, these may vary independently from dwell to dwell.

Let $\mathbf{W}_{d,0}$ denote the interference term in (1). Since the elements of $\boldsymbol{x}_{d,i}$ are zero-mean and independent, the same holds for the elements of $\mathbf{W}_{d,0}$. Moreover, provided that $[\boldsymbol{x}_{d,i}]_t$ is selected from a PSK constellation of unit power, $\mathrm{e}^{\mathrm{i}\phi_i}[\boldsymbol{h}_{d,i}]_n[\boldsymbol{x}_{d,i}]_t \sim \mathcal{CN}(0,1)$, $n = 1, \ldots, N$, $t = 1, \ldots, T_d$. Given $\{e_{d,i}, r_i\}$, it follows that $[\mathbf{W}_{d,0}]_{n,t} \sim \mathcal{CN}(0, I_{d,0})$, where $I_{d,0} \triangleq \sum_{i\neq 0} e_{d,i} r_i^{-b}$ is the interference power seen by $\mathrm{RX}_0$ in dwell $d$. In the case of QAM constellations, we approximate $[\mathbf{W}_{d,0}]_{n,t}$ as Gaussian for the sake of tractability.

$\mathrm{RX}_0$ can obtain knowledge of $\boldsymbol{h}_{d,0}$ and $I_{d,0}$ with the help of pilot symbols which are transmitted at the beginning of the dwell. Presently, we assume that they are perfectly known; a straightforward channel estimation algorithm is presented in Section V.

[3]We assume that the encoder is trellis-terminated [13], i.e., it is forced to start from and end at the zero-state. This results in a small rate loss which is not taken into account.

[4]For convenience, we assume that $L_\mathrm{b}/(R_c M_c)$ and $D$ are integer.

[5]In reality, the hopping pattern is determined pseudorandomly and is known at the RX. The model of random FH is convenient for analytical purposes.

[6]We assume that the average received power $R^{-b}$ per antenna is known at $\mathrm{RX}_0$. We have taken it into account in the interference portion of the received signal because it is convenient in terms of notation.

### B. Equivalent channel model and decoding

The reference RX performs MRC, i.e., it evaluates the product $\frac{\boldsymbol{h}_{d,0}^{\mathrm{H}}}{\|\boldsymbol{h}_{d,0}\|^2}\mathbf{Y}_{d,0}$. From (1), we have

$$\frac{\boldsymbol{h}_d^{\mathrm{H}}}{\|\boldsymbol{h}_d\|^2}\mathbf{Y}_d = \boldsymbol{x}_d^{\mathrm{T}} + \frac{\boldsymbol{h}_d^{\mathrm{H}}}{\|\boldsymbol{h}_d\|^2}\mathbf{W}_d, \qquad (2)$$

where we have omitted the index 0 in order to simplify the notation. Denoting the $t^{\mathrm{th}}$ columns of $\mathbf{Y}_d$ and $\mathbf{W}_d$ as $\boldsymbol{y}_t$ and $\boldsymbol{w}_t$, respectively, we have the following equivalent channel model for data symbol $x_k$, $k = (d-1)T_d + 1, \ldots, dT_d$, which is transmitted in dwell $d$

$$y_k = x_k + w_k, \qquad (3)$$

where $y_k = \frac{\boldsymbol{h}_d^{\mathrm{H}}}{\|\boldsymbol{h}_d\|^2}\boldsymbol{y}_t$ and $w_k = \frac{\boldsymbol{h}_d^{\mathrm{H}}}{\|\boldsymbol{h}_d\|^2}\boldsymbol{w}_t$. Since $\boldsymbol{w}_t \sim \mathcal{CN}(0, I_d\mathbf{I}_N)$, it follows that $w_k \sim \mathcal{CN}(0, \gamma_k^{-1})$, given the equivalent SIR $\gamma_k = \frac{\|\boldsymbol{h}_d\|^2}{I_d}$, where, by definition, $d = \lceil \frac{k}{T_d} \rceil$. The r.v. $a_d = \|\boldsymbol{h}_d\|^2$ is chi-square distributed with $2N$ degrees of freedom, i.e., $a_d \sim \chi^2_{2N}$. In addition, due to the fact that the locations of the inteferers in each dwell are a realization of a Poisson point process with density $\lambda/M$, it is known that $I_d$ is an $\alpha$-stable r.v. with stability exponent $\alpha = 2/b$ [12], [14]. Its moment generating function (mgf) is [12]

$$\Phi_I(s) = \mathbb{E}[\mathrm{e}^{-Is}] = \mathrm{e}^{-\frac{\lambda\delta}{M}s^\alpha}, \quad s > 0, \qquad (4)$$

where

$$\delta \triangleq \pi\Gamma(1-\alpha)R^2 \qquad (5)$$

and $\Gamma(\zeta)$, $\zeta > 0$, denotes the gamma function. The sequence $\{y_k, \gamma_k\}_{k=1}^{DT_d}$ is the input to the decoder which decides that the codeword $\hat{\boldsymbol{c}}$ was transmitted according to the simplified maximum-likelihood (ML) criterion [5, Eq. (9)]

$$\hat{\boldsymbol{c}} = \arg\min_{\boldsymbol{c}} \sum_{\substack{k'=1 \\ k' \leftrightarrow (k, j_{k'})}}^{L_\mathrm{b}/R_c} \gamma_k \min_{x \in \mathcal{X}_{c_{k'}}^{j_{k'}}} \left\{ |y_k - x|^2 \right\}, \qquad (6)$$

where $\mathcal{X}_{c_{k'}}^{j_{k'}}$ denotes the set of constellation symbols that have bit $c_{k'}$ at position $j_{k'}$, $j_{k'} = 1, \ldots, M_c$. The weighting of each distance metric by the respective SIR reflects the confidence of the decoder in that metric. Note that the summation is over the bit index $k'$, which corresponds to a unique pair $(k, j_{k'})$ through the interleaver mapping.

## III. Analysis

This section is devoted to the performance analysis of decoder (6). In order to round out the analysis, in Section III-D, we also derive upper and lower bounds to the ergodic capacity of channel (3). Since the scheme presented in Section II induces an "averaging" over different channel states within the packet, the ergodic capacity is an upper bound to the information rate of the typical TX-RX link.

### A. Decoder performance

The codeword (or frame) error probability (FEP) of decoder (6), $P_e$, is upper-bounded as [13]

$$P_e \leq L_{\rm b} \sum_{l=L,L+1,\ldots} w_l P_l, \tag{7}$$

where $P_l$ is the probability of a length-$l$ error event, or pairwise error probability, and $w_l$ is the number of length-$l$ error events. The minimum length of an error event $L$, i.e., the Hamming distance, as well as the weight distribution $\{w_l\}$ depend on the particular code employed.

We now assume that, due to random interleaving, the sequence of $l$ symbols that correspond to a sequence of $l$ coded bits encounter *independent* SIR conditions (this assumption is discussed in Section V). From [5], [15], $P_l$ can be upper-bounded by

$$\bar{P}_l = \frac{1}{\pi}\int_0^{\pi/2}\left(\frac{1}{M_c 2^{M_c}}\sum_{(x,x')\in\mathcal{X}}\Phi_\gamma\left(\frac{|x-x'|^2}{4\sin^2\theta}\right)\right)^l \mathrm{d}\theta, \tag{8}$$

where $\Phi_\gamma(s) = \mathbb{E}[\mathrm{e}^{-\gamma s}]$, $s > 0$. (The time index $k$ has been removed as it is of no consequence.) $(x, x')$ are all possible $M_c 2^{M_c}$ nearest-neighbor pairs in $\mathcal{X}$ which have complementary bits in position $j$, $j = 1, \ldots, M_c$, e.g., for QPSK constellations with Gray mapping, all such pairs are at the minimum constellation distance $d_{\min}$. Note that, in the limit of large $E[\gamma]$, the bound is tight, i.e., $\bar{P}_l \simeq P_l$ [5].

From (7), a further upper bound to $P_e$ is

$$\bar{P}_e = L_{\rm b} \sum_{l=L,L+1,\ldots} w_l \bar{P}_l. \tag{9}$$

The evaluation of $\bar{P}_l$ in (8) is possible by numerical integration, provided that $\Phi_\gamma(s)$ is known. The derivation of $\Phi_\gamma(s)$ is the topic of the following subsection.

### B. Statistics of $\gamma$

The probability density function (pdf) of $\gamma$ is given by the following lemma.

**Lemma 1** *The pdf of the SIR $\gamma$ is*

$$f_\gamma(x) = \frac{1}{(N-1)!}\frac{\mathrm{e}^{-\frac{\lambda\delta}{M}x^\alpha}}{x}\sum_{n=1}^{N}\frac{|\beta_n^N|}{n!}\left(\frac{\lambda\delta}{M}x^\alpha\right)^n, \tag{10}$$

*$x > 0$, where*

$$\beta_n^N = \sum_{m=1}^{n}(-1)^m \binom{n}{m} (\alpha m)_N,\ n = 1, \ldots, N \tag{11}$$

*and $(\alpha m)_N \triangleq \alpha m \ldots (\alpha m - N + 1)$ is the falling sequential product.*

*Proof:* The cumulative distribution function (cdf) of $\gamma$, $F_\gamma(x)$, is by definition

$$F_\gamma(x) = \mathbb{P}(a \leq xI) = \int_0^{+\infty} F_a(xy) f_I(y)\mathrm{d}y, \tag{12}$$

where

$$F_a(x) = 1 - \mathrm{e}^{-x}\sum_{n=0}^{N-1}\frac{x^n}{n!} = 1 - \frac{\Gamma(N,x)}{(N-1)!},\quad x > 0 \tag{13}$$

is the cdf of $a$ and $\Gamma(\zeta, x) = \int_x^{+\infty}\mathrm{e}^{-t}t^{\zeta-1}\mathrm{d}t$, $x \geq 0$, is the incomplete gamma function. Substituting (13) in (12) and taking the derivative, the pdf of $\gamma$ is given by

$$\begin{aligned} f_\gamma(x) &= -\frac{1}{(N-1)!}\int_0^{+\infty}\frac{\mathrm{d}\Gamma(N,xy)}{\mathrm{d}x} f_I(y)\mathrm{d}y \\ &= \frac{x^{N-1}}{(N-1)!}\int_0^{+\infty} f_I(y) y^N \mathrm{e}^{-xy}\mathrm{d}y \\ &= \frac{(-1)^N x^{N-1}}{(N-1)!}\frac{\mathrm{d}^N\Phi_I(x)}{\mathrm{d}x^N}, \end{aligned} \tag{14}$$

where we have used the identity $\frac{\mathrm{d}\Gamma(\zeta,x)}{\mathrm{d}x} = -x^{\zeta-1}\mathrm{e}^{-x}$ [16, p. 951] and the Laplace transform property[7]

$$f_I(y)y^N \overset{\mathcal{L}}{\longleftrightarrow} (-1)^N\frac{\mathrm{d}^N\Phi_I(s)}{\mathrm{d}s^N}.$$

From the identity for the $N^{\rm th}$ derivative of a composite function [16, Eq. (0.430.1), p. 24], after some algebra we obtain

$$\frac{\mathrm{d}^N\Phi_I(s)}{\mathrm{d}s^N} = s^{-N}\mathrm{e}^{-\frac{\lambda\delta}{M}s^\alpha}\sum_{n=1}^{N}\frac{\beta_n^N}{n!}\left(\frac{\lambda\delta}{M}s^\alpha\right)^n \tag{15}$$

with $\beta_n^N$ given by (11). From (15) and (14)

$$f_\gamma(x) = \frac{1}{(N-1)!}\frac{\mathrm{e}^{-\frac{\lambda\delta}{M}x^\alpha}}{x}\sum_{n=1}^{N}\frac{(-1)^N\beta_n^N}{n!}\left(\frac{\lambda\delta}{M}x^\alpha\right)^n. \tag{16}$$

In order to derive (10) from (16), we need to show that $(-1)^N\beta_n^N \geq 0$. Once again, using the identity for the $N^{\rm th}$ derivative of a composite function, $\beta_n^N$ can be written as the following derivative evaluated at $x = 1$:

$$\beta_n^N = \left.\frac{\mathrm{d}^N\left(1-x^\alpha\right)^n}{\mathrm{d}x^N}\right|_{x=1} \tag{17}$$

From (17), the following iterative relation can be proved for $N \geq 2$

$$\beta_n^N = \sum_{m_1=1}^{N}\binom{N}{m_1}\beta_1^{m_1}\beta_{n-1}^{N-m_1}. \tag{18}$$

By successive application of (18), we obtain

$$\begin{aligned} &\frac{(-1)^N\beta_n^N}{N!} = \\ &\sum_{m_1=1}^{N}\cdots\sum_{m_{n-1}=1}^{N-m_{n-2}-\cdots-m_1}(-1)^{m_1}\beta_1^{m_1}\ldots(-1)^{m_n}\beta_1^{m_n}, \end{aligned}$$

where $m_n = N - m_{n-1} - \cdots - m_1$. Due to (11), $(-1)^N\beta_1^N = (-1)^{N+1}\alpha(\alpha-1)\ldots(\alpha-N+1)$. Since $\alpha = 2/b < 1$, it follows that $(-1)^N\beta_1^N \geq 0$. Therefore, $(-1)^N\beta_n^N \geq 0$ for $n = 1, \ldots, N$. ∎

As expected, increasing the spatial diversity order $N$ increases the value of $f_\gamma(x)$, as more positive terms are added to the polynomial in (10). Eq. (10) enables the numerical evaluation of $\Phi_\gamma(s)$ using Gauss-Laguerre quadrature for any $s > 0$.

[7] This identity is also employed in [17], in order to derive the ccdf of $\gamma$.

### C. Approximations

The numerical evaluation of $\bar{P}_l$ from (8) does not provide insight on how the decoder performance depends on the system parameters. In this section, we examine the decoder performance when $\lambda/M \to 0$, i.e., the interferer point process in each dwell is sparse. This implies that the network is operated in a regime of small FEP, i.e., typically $\bar{P}_e \leq \epsilon$, with $\epsilon \leq 0.1$.

Let $B(\zeta_1, \zeta_2),\ \zeta_1, \zeta_2 > 0$ denote the beta function. Our main result is stated in the following proposition.

**Proposition 1** *If $\lambda/M \to 0$, then $\bar{P}_l = \eta(\frac{\lambda}{M})^l + o\left(\left(\frac{\lambda}{M}\right)^l\right)$, where $\bar{P}_l$ is defined in (8) and $\eta$ is a positive constant. Moreover,*

$$\bar{P}_l \simeq \frac{2^{4\alpha l-1}}{\pi} B\left(\alpha l + \frac{1}{2}, \alpha l + \frac{1}{2}\right) \left(\frac{\alpha B(N-\alpha,\alpha)}{d_{\mathcal{X}}^2} \frac{\lambda \pi R^2}{M}\right)^l \tag{19}$$

*where*

$$d_{\mathcal{X}}^2 = \left(\frac{1}{M_c 2^{M_c}} \sum_{(x,x')\in\mathcal{X}} \frac{1}{|x-x'|^{2\alpha}}\right)^{-1}. \tag{20}$$

*Proof:* Omitting the term $\mathrm{e}^{-\frac{\lambda\delta}{M}x^\alpha}$ in (10), an upper bound to $\Phi_\gamma(s)$ for all $s > 0$ is

$$\begin{aligned}\overline{\Phi_\gamma(s)} &= \frac{1}{(N-1)!} \sum_{n=1}^{N} \frac{|\beta_n^N|}{n!} \left(\frac{\lambda\delta}{M}\right)^n \int_0^{+\infty} x^{\alpha n-1} \mathrm{e}^{-xs} \mathrm{d}x \\ &= \frac{1}{\Gamma(N)} \sum_{n=1}^{N} \frac{|\beta_n^N|}{n!} \left(\frac{\lambda\delta}{M}\right)^n s^{-\alpha n} \Gamma(\alpha n) \\ &= \frac{\alpha B(N-\alpha,\alpha)}{\Gamma(1-\alpha)} \left(\frac{\lambda\delta}{M}\right) s^{-\alpha} \\ &\quad + \frac{1}{\Gamma(N)} \sum_{n=2}^{N} \frac{|\beta_n^N|}{n!} \left(\frac{\lambda\delta}{M}\right)^n s^{-\alpha n} \Gamma(\alpha n). \end{aligned} \tag{21}$$

Eq. (21) is derived by successively applying the identity $\Gamma(\zeta+1) = \zeta\Gamma(\zeta)$ to show that

$$|\beta_1^N| = \alpha(1-\alpha)\dots(N-1-\alpha) = \frac{\alpha}{\Gamma(1-\alpha)}\Gamma(N-\alpha)$$

and the definition of the beta function

$$B(N-\alpha,\alpha) = \frac{\Gamma(N-\alpha)\Gamma(\alpha)}{\Gamma(N)}, \tag{22}$$

where $\Gamma(N) = (N-1)!$. From (21) and (8), we can see that $\bar{P}_l = \eta\left(\frac{\lambda}{M}\right)^l + o\left(\left(\frac{\lambda}{M}\right)^l\right)$, for $\lambda/M \to 0$, with $\eta$ appropriately defined.

Note that the bound in (21) is tight as $\lambda/M \to 0$. Ignoring the higher order terms and recalling the definition of $\delta$ in (5)

$$\Phi_\gamma(s) \simeq \overline{\Phi_\gamma(s)} \simeq \pi\alpha R^2 B(N-\alpha,\alpha) s^{-\alpha} \frac{\lambda}{M}. \tag{23}$$

Substituting (23) in (8)

$$\bar{P}_l \simeq \left(\pi\alpha R^2 B(N-\alpha,\alpha) d_{\mathcal{X}}^{-2} \frac{\lambda}{M}\right)^l \frac{4^{\alpha l}}{\pi} \int_0^{\pi/2} (\sin\theta)^{2\alpha l}\ \mathrm{d}\theta,$$

where $d_{\mathcal{X}}^2$ is defined in (20). Employing the identity [16, p. 412]

$$\int_0^{\pi/2} (\sin\theta)^{2\alpha l}\ \mathrm{d}\theta = 2^{2\alpha l-1} B(\alpha l + 1/2, \alpha l + 1/2)$$

we obtain (19). ∎

*Remarks:* Proposition 1 states that for $\lambda/M \to 0$ the Hamming distance of the convolutional code determines the *diversity order*, i.e., the slope of the curve of $\bar{P}_e$ vs. $\lambda/M$ in log-log coordinates. This result is reminiscent of the performance of BICM in a Rayleigh fading channel with AWGN. The difference is that, in the context of an inteference-limited random network, the average signal-to-noise ratio is replaced by $N_{\text{eff}}^{-1}$, where $N_{\text{eff}} = \frac{\lambda\pi R^2}{M}$ is the expected number of TXs in the transmission range per subband.

Eq. (19) also reveals that MRC introduces an array or *coding* gain through the factor $B(N-\alpha,\alpha)^L$. To obtain further insight, we examine the trend of the beta function for large $N$. By Stirling's approximation, for large $\zeta$ we have $\Gamma(\zeta) \simeq \sqrt{2\pi}\zeta^{\zeta-1/2}\mathrm{e}^{-\zeta}$, therefore

$$\frac{\Gamma(N-\alpha)}{\Gamma(N)} \simeq N^{-\alpha}\left(1-\frac{\alpha}{N}\right)^{N-\alpha-\frac{1}{2}} \mathrm{e}^{\alpha}.$$

However, it is easy to verify that $\lim_{N\to\infty}\left(1-\frac{\alpha}{N}\right)^{N-\alpha-\frac{1}{2}} = \mathrm{e}^{-\alpha}$, so, from (22), $B(N-\alpha,\alpha) \simeq \Gamma(\alpha)N^{-\alpha}$. As a result, for large $N$, the coding gain is proportional to $N^{-L\alpha}$.

A final observation is that, similarly to [5], the parameter $d_{\mathcal{X}}^2$ is the harmonic mean of the minimum squared Euclidean distance between the nearest-neighbor pairs defined in Section III-A, raised to the stability exponent $\alpha$.

### D. Ergodic capacity

The ergodic capacity of (3) is

$$C = \int_0^{+\infty} f_\gamma(x) \log_2(1+x) \mathrm{d}x. \tag{24}$$

A closed form expression appears hard to obtain due to the complicated nature of (10); nevertheless, the integral can be evaluated numerically with Gauss-Laguerre quadrature. The following proposition provides upper and lower bounds on $C$.

**Proposition 2** *The ergodic capacity of (3) is upper-bounded as*

$$C < \bar{C} = \log_2\left(1 + N\Gamma\left(\frac{1}{\alpha}+1\right)\left(\frac{M}{\lambda\delta}\right)^{1/\alpha}\right) \tag{25}$$

*and lower bounded as*

$$C \geq \underline{C} = \frac{1}{\alpha}\log_2\left(\frac{M}{\mathrm{e}^\Gamma \lambda\delta}\right) + \frac{H_{N-1}}{\ln 2}, \tag{26}$$

*where $\Gamma = 0.577\dots$ is the Euler-Mascheroni constant and*

$$H_n = \begin{cases} \sum_{k=1}^{n} \frac{1}{k} & n \geq 1 \\ 0 & n = 0 \end{cases} \tag{27}$$

*is the $n^{\text{th}}$ harmonic number. This bound is tight, i.e., $C \simeq \underline{C}$ for $\lambda \to 0$. A looser lower bound is*

$$\underline{\underline{C}} = \frac{1}{\alpha} \log_2 \left( \frac{N^\alpha M}{\mathrm{e}^\Gamma \lambda \delta} \right). \tag{28}$$

*Proof:* The upper bound is derived by noting that $\mathbb{E}[\gamma] = \mathbb{E}[a]\mathbb{E}\left[\frac{1}{I}\right] = N\mathbb{E}\left[\frac{1}{I}\right]$, so, for $N = 1$, $\mathbb{E}\left[\frac{1}{I}\right] = \mathbb{E}[\gamma]$. Setting $N = 1$ in (10), we have

$$\mathbb{E}\left[\frac{1}{I}\right] = \frac{\lambda\delta\alpha}{M} \int_0^{+\infty} x^\alpha \mathrm{e}^{-\frac{\lambda\delta}{M}x^\alpha} \mathrm{d}x = \left(\frac{M}{\lambda\delta}\right)^{1/\alpha} \Gamma\left(\frac{1}{\alpha}+1\right).$$

By applying Jensen's inequality[8] on (24), we obtain (25).

For the derivation of the lower bound, we employ the inequality $\ln(1+x) > \ln x$ for $x > 0$. Combining (14) and (24) and integrating by parts, we obtain

$$\begin{aligned}((N-1)!\ln 2)\,\underline{C} &= (-1)^N \int_0^{+\infty} x^{N-1} \left(\Phi_I(x)\right)^{(N)} \ln x \mathrm{d}x \\ &= (-1)^N \sum_{k=0}^{N-2} (-1)^k \left[ \left(\Phi_I(x)\right)^{(N-k-1)} \left(x^{N-1}\ln x\right)^{(k)} \right]_0^{+\infty} \\ &\quad - \int_0^{+\infty} \left(\Phi_I(x)\right)^{(1)} \left(x^{N-1}\ln x\right)^{(N-1)} \mathrm{d}x. \end{aligned} \tag{29}$$

For convenience, the notation $\left(\Phi_I(x)\right)^{(n)}$ has been adopted to denote the $n^{\text{th}}$ derivative of $\Phi_I(x)$ and likewise for the other functions. After some algebra, we can show that, for $k = 1, \ldots, N-1$, $N > 1$,

$$\begin{aligned}\left(x^{N-1}\ln x\right)^{(k)} &= (N-1)\ldots(N-k)x^{N-k-1}\ln x \\ &\quad + x^{N-k-1} \sum_{(l_1,\ldots,l_{k-1})} (N-l_1)\ldots(N-l_{k-1}), \end{aligned} \tag{30}$$

with the summation taken over all permutations of the vector $(l_1, \ldots, l_{k-1})$, $l_j = 1, \ldots, k$, $j = 1, \ldots, k-1$. When $k = N-1$

$$\left(x^{N-1}\ln x\right)^{(N-1)} = (N-1)!(\ln x + H_{N-1}), \tag{31}$$

where $H_n$ is defined in (27). From (15) and (30), we can show that the first term in (29) is zero. Hence

$$\underline{C} = \frac{\lambda\delta\alpha}{M\ln 2} \int_0^{+\infty} x^{\alpha-1} \mathrm{e}^{-\frac{\lambda\delta}{M}x^\alpha} \ln x \; \mathrm{d}x + \frac{H_{N-1}}{\ln 2},$$

from which (26) follows by use of [16, Eq. (4.331.1), p. 602].

Since the harmonic number is lower bounded as [19]

$$H_N > \ln N + \Gamma + \frac{1}{2(N+1)},$$

for $N \geq 2$, we have that

$$H_{N-1} = H_N - \frac{1}{N} > \ln N + \Gamma + \frac{1}{2(N+1)} - \frac{1}{N} > \log N.$$

The latter inequality holds because, for $N \geq 2$, $\frac{1}{N} - \frac{1}{2(N+1)} < \frac{1}{2} < \Gamma$, $\forall N \geq 2$. As a result, a looser lower bound to the capacity is (28). ∎

Eq. (28) shows that $\underline{C}$ is a linear function of $\log_2\left(\frac{M}{\lambda\delta}\right)$, with slope $1/\alpha = b/2$ and a constant term $\log_2 N - \frac{\Gamma}{\alpha}\log_2 \mathrm{e}$.

[8]Jensen's inequality was also employed in [18] in order to derive an upper bound to the ergodic capacity, albeit in a slightly different context.

## IV. Network metrics

Having evaluated the performance at the link level, we now turn our attention to network-wide metrics. The network thoughput per unit area is defined as the spatial density of successful transmissions multiplied by their rate $R_c M_c$, i.e.,

$$\tau = \lambda(1 - P_e) R_c M_c.$$

Similarly to [2], the transmission capacity $\tau_\epsilon$ is defined as the maximum network throughput per unit area such that a constraint $P_e = \epsilon$ is satisfied, i.e.,

$$\tau_\epsilon = \lambda_\epsilon (1-\epsilon) R_c M_c, \tag{32}$$

where $\lambda_\epsilon$ is the maximum contention density. A closed-form expression for $\lambda_\epsilon$ may be obtained by noting that, for $\epsilon \to 0$, the Hamming distance error events dominate the FEP, i.e., $P_e \simeq \bar{P}_e \simeq L_{\mathrm{b}} w_L \bar{P}_L$. From Proposition 1, we find that

$$\lambda_\epsilon \approx \left(\frac{\epsilon}{K}\right)^{1/L} \frac{d_{\mathcal{X}}^2 M}{16^\alpha \alpha B(N-\alpha,\alpha)\pi R^2}, \tag{33}$$

where

$$K \triangleq \frac{L_{\mathrm{b}} w_L}{2\pi} B(\alpha L + 1/2, \alpha L + 1/2). \tag{34}$$

The maximum contention density is therefore proportional to $\epsilon^{1/L}$, as $\epsilon \to 0$. This result is a manifestation of the channel diversity harnessed through FH and coding at the expense of spectrum. As seen from (33) and (34), the proportionality constant depends, among other system parameters, on the selected code, i.e., $L$ and $w_L$, the codeword length $L_{\mathrm{b}}$, the geometry of the symbol constellation and the number of RX antennas $N$. Since $B(N-\alpha,\alpha) \approx N^{-\alpha}$ for increasing $N$, it also follows that $\lambda_\epsilon$ is proportional to $N^\alpha$, which is in agreement with the scaling law derived in [17].

As a final note, the network throughput is upper-bounded by $\bar{\tau} = \lambda C$, where $C$ is the link ergodic capacity given by (24). Bounds on $\bar{\tau}$ may be obtained by employing the results of Proposition 2.

## V. Physical-layer considerations

This section discusses various physical-layer issues with respect to the system model presented in Section II. The influence of these on the decoder performance is assessed via simulation in Section VI.

### A. Channel estimation

In this subsection, we discuss the important issue of how the decoder obtains estimates of $\boldsymbol{h}_d$ and $I_d$ in the $d^{\text{th}}$ dwell. Assume that a header of $T_p$ pilot symbols, selected from a complex PSK constellation of zero mean and unit power, and known at the RX, is transmitted at the beginning of the dwell. If this header is denoted as $\boldsymbol{p}_d^{\mathrm{T}}$, then, similarly to (1), the received pilot matrix is

$$\mathbf{Y}_d = \boldsymbol{h}_d \boldsymbol{p}_d^{\mathrm{T}} + \mathbf{W}_d$$

where $\mathbf{W}_d = R^{b/2} \sum_{i \neq 0} e_{d,i} r_i^{-b/2} \mathrm{e}^{\mathrm{i}\phi_i} \boldsymbol{h}_{d,i} \boldsymbol{p}_{d,i}^{\mathrm{T}}$ and $[\mathbf{W}_d]_{n,t}$, $n = 1, \ldots, N$, $t = 1, \ldots, T_p$ are i.i.d. with $[\mathbf{W}_d]_{n,t} \sim \mathcal{CN}(0, I_d)$, given $I_d$.

An estimate of $I_d$ is

$$\hat{I}_d = \frac{1}{N(T_p-1)} \left\| \left( \mathbf{I}_T - \frac{1}{T_p} \boldsymbol{p}_d \boldsymbol{p}_d^{\mathrm{H}} \right) \mathbf{Y}_d^{\mathrm{T}} \right\|^2,$$

obtained by finding jointly the ML estimators of $\boldsymbol{h}_d$ and $I_d$ [20, p. 182] and multiplying the latter by the factor $T_p/(T_p-1)$ in order to remove the bias. Intuitively, the estimate of the interference power is obtained by projecting the received signal onto the subspace which is orthogonal to the pilot data $\boldsymbol{p}$. Assuming that the estimate of $I_d$ is accurate, i.e., $\hat{I}_d \approx I_d$, the minimum mean-square error (MMSE) estimate of $\boldsymbol{h}_d$ is [20, p. 391]

$$\hat{\boldsymbol{h}}_d = \frac{1}{I_d + T_p} \mathbf{Y}_d \boldsymbol{p}_d^*.$$

Defining $\boldsymbol{\epsilon}_d = \boldsymbol{h}_d - \hat{\boldsymbol{h}}_d$, it holds that $\hat{\boldsymbol{h}}_d \sim \mathcal{CN}\left(\mathbf{0}, \frac{T_p}{I_d+T_p}\mathbf{I}_N\right)$, $\boldsymbol{\epsilon}_d \sim \mathcal{CN}\left(\mathbf{0}, \frac{I_d}{I_d+T_p}\mathbf{I}_N\right)$ and $\hat{\boldsymbol{h}}_d, \boldsymbol{\epsilon}_d$ are independent. We can see that the estimate of $\boldsymbol{h}_d$ is accurate if $T_p \gg I_d$.

Following the estimation of $\boldsymbol{h}_d$ and $I_d$, the RX performs MRC, i.e., it evaluates the product $\frac{\hat{\boldsymbol{h}}_d^{\mathrm{H}}}{\|\hat{\boldsymbol{h}}_d\|^2}\mathbf{Y}_d$. From (1), we have

$$\frac{\hat{\boldsymbol{h}}_d^{\mathrm{H}}}{\|\hat{\boldsymbol{h}}_d\|^2}\mathbf{Y}_d = \boldsymbol{x}_d^{\mathrm{T}} + \frac{\hat{\boldsymbol{h}}_d^{\mathrm{H}}}{\|\hat{\boldsymbol{h}}_d\|^2}\left(\boldsymbol{\epsilon}_d \boldsymbol{x}_d^{\mathrm{T}} + \mathbf{W}_d\right).$$

Lumping the channel estimation error term with the interference, we can show that the equivalent channel model follows (3), with the SIR defined as

$$\gamma_{k,\mathrm{csi}} = \frac{a_d}{I_d}\left(1 + \frac{1+I_d}{T_p}\right)^{-1}.$$

The sequence $\{y_k, \gamma_{k,\mathrm{csi}}\}_{k=1}^{DT_d}$ is the input to decoder (6).

A consequence of channel estimation is the loss of information rate by a factor $\frac{T_d}{T_d+T_p}$, due to the transmission of the pilot symbols in each dwell. This factor must be taken into account when evaluating the transmission capacity.

### B. Correlation of the interference

Eq. (8) is based on the assumption that the coded bits encounter independent SIR conditions across the span of an error event in the decoder. The assumption is justified if, (a) there is a sufficient number of dwells[9] such that, due to interleaving, these bits will be transmitted on different dwells, and (b) the SIRs are independent across dwells. The latter assumption is reasonable if the number of frequencies is sufficiently large. As shown in [21], the temporal correlation of the interference in a fixed Poisson network of TXs and Rayleigh fading is $p/2$, where $p$ is the random access probability. In this paper, random access is achieved via random FH, i.e., $p$ can be substituted by $1/M$.

[9]This is also related to the length of the codeword.

### C. Synchronization

The assumption of synchronization between different TX-RX pairs in the network facilitates the analysis, as the interference power is the same throughout each dwell. We anticipate that the results of our analysis will also hold in the case of asynchronous transmissions, provided that the interference power can be estimated accurately. This may necessitate the insertion of more pilot symbols throughout the dwell and, consequently, the loss of rate. The study of these issues is beyond the scope of the present paper.

### D. Power control

In [2], it was shown that channel-inversion PC increases the outage probability in a random network with fading. In order to examine the effect of PC in the context of this paper, we assume that the typical TX-RX link is subject to lognormal shadowing, i.e., the transmitted signal is multiplied by a r.v. $S = 10^{\sigma_s \xi/10}$, where $\xi \sim \mathcal{N}(0,1)$ and, typically, $\sigma_s = 6-8$ dB. Note that $S$ (like the node locations) is assumed to be a "long-term" r.v., i.e., it is constant for at least the duration of a packet slot.

In order to take shadowing into account in the analysis of Section III, the definition of the constant $\delta$ in (5) for the case of channel-inversion PC must be modified as $\delta_{\mathrm{pc}} = \pi\Gamma(1-\alpha)R^2\mathbb{E}[(S^\alpha S'^{-\alpha}]$, where $S$ models the shadowing between $\mathrm{TX}_i$ and $\mathrm{RX}_0$ and $S'$ models the shadowing between $\mathrm{TX}_i$ and its corresponding RX. In the absence of PC, we have $\delta_{\mathrm{npc}} = \pi\Gamma(1-\alpha)R^2\mathbb{E}[S^\alpha]S'^{-\alpha}$, where $S'$ now denotes the shadowing between $\mathrm{TX}_0$ and $\mathrm{RX}_0$. Therefore, in the case of no PC, $P_l$ in (8) is conditioned on the realization of $S'$ and the expectation of the former with respect to the latter must be taken in order to obtain the unconditional probability of codeword/packet error.

## VI. Numerical results

In this section, we present numerical results for a network with default parameters $R = 1$ m, $M = 100$, $M_c = 2$ (QPSK), $N = 2$ and $b = 4$. Six convolutional codes with rate $R_c = 1/2$ are considered, with memory, minimum Hamming distances and distance spectra listed in Table II (see [22] for more details). In all plots, the upper bound to the pairwise error probability $\bar{P}_l$ is evaluated by (19).

In the simulations, we generate a new network realization for every transmitted packet. The network area is selected such that, on average, there are $60$ interferers per subband. At the TX, we employ a block interleaver of vertical dimension equal to the number of bits per dwell $M_c T_d$ and horizontal

TABLE II
Optimum rate 1/2 convolutional codes

| Encoder | Memory | $L$ | $w_L, \ldots, w_{L+4}$ |
|---|---|---|---|
| Enc1 | 1 | 3 | 1,1,1,1,1 |
| Enc2 | 2 | 4 | 2,0,5,0,13 |
| Enc3 | 3 | 5 | 1,0,6,0,16 |
| Enc4 | 3 | 6 | 1,3,5,11,25 |
| Enc5 | 5 | 8 | 2,7,10,18,49 |
| Enc6 | 7 | 10 | 1,6,13,20,64 |

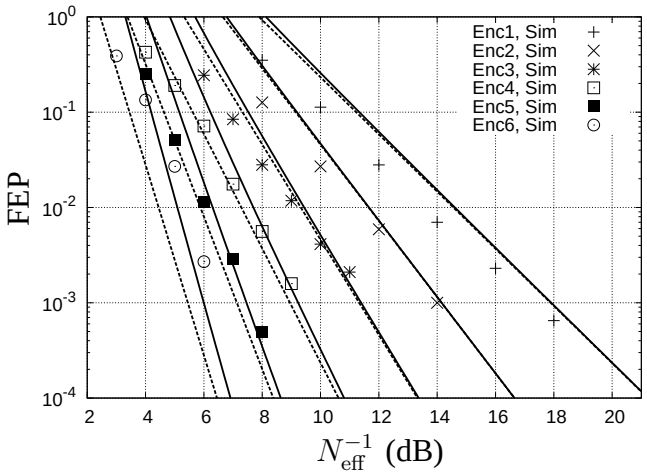


Fig. 1. FEP vs. $N_{\rm eff}^{-1}$ for the codes in Table II. The solid (dotted) lines depict (9) with error events up to length $L+4$ ($L$) taken into account. The theoretical result is slightly optimistic in the case of Enc6. This is attributed to the impact of channel correlation within the packet, the effect of which becomes more apparent as the span of the error events becomes larger (QPSK, $L_{\rm b} = 800$, $D = 40$, $T_d = 20$, $N = 2$, $b = 4$, perfect CSI).

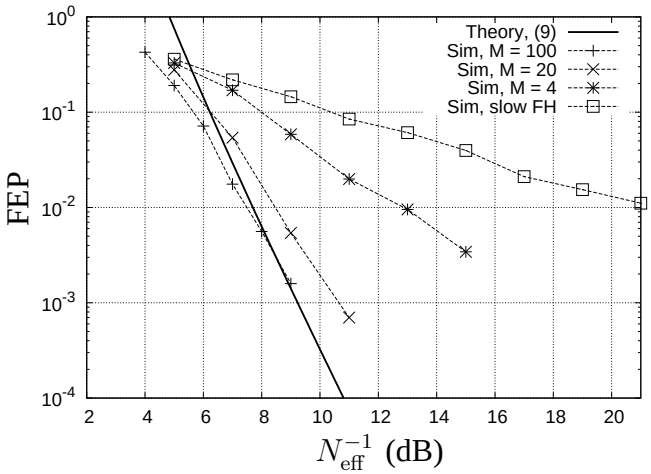


Fig. 2. FEP vs. $N_{\rm eff}^{-1}$ for Enc4 and $M = 4, 20, 100$. As $M$ decreases the diversity order decreases, as the fading and interference across dwells become more correlated. The simulated performance for slow FH is also shown for comparison (QPSK, $L_{\rm b} = 800$, $D = 40$, $T_d = 20$, $N = 2$, $b = 4$, perfect CSI).

dimension equal to $D$, such that $D$ consecutive codeword bits are guaranteed to be transmitted on different dwells. The coherence time of the fading is taken to be equal to the duration of a packet. In this manner, we can compare the scheme proposed in this paper with the slow-FH (IA) scheme advocated in [6].

In Fig. 1, we plot the FEP vs. $N_{\rm eff}^{-1}$ (recall that $N_{\rm eff}$ is the expected number of TXs in a disc of radius $R$ per subband) for the codes listed in Table II and $L_{\rm b} = 800$. The upper bound (9) is plotted with a solid line, when error events up to length $L + 4$ are taken into account, and with a dotted line, when only the Hamming distance error events are taken into account. As expected, for each code, the two curves converge as $N_{\rm eff} \to 0$. We also simulate the performance of the codes by dividing the packet in $D = 40$ dwells of $T_d = 20$ QPSK symbols. Fig. 1 demonstrates that the dotted curve is quite accurate for $P_e < 0.01$.

In Fig. 2, we investigate for what range of values of $M$ channel conditions across dwells can be considered independent. We obtain the FEP of Enc4 via simulation for different systems which have the same $N_{\rm eff}$ but varying $M$. It is observed that, for $M \geq 20$, full diversity can practically be attained, as the simulated curves are very close to the theoretical one which is derived based on the assumption of independent channels. The simulated FEP in the case of slow FH is also shown for comparison. Note that, given $N_{\rm eff}$, the performance of slow FH does not depend on $M$; its diversity order is always one.

In Fig. 3, we plot the maximum contention density $\lambda_\epsilon$, evaluated by (33), vs. $L$, for the set of parameters of Fig. 1 and different values of the ratio $\epsilon/w_L$. Note that, for $\epsilon/w_L = 0.001$, increasing the diversity order of the code from 3 to 8, results in a tenfold increase of $\lambda_\epsilon$. The gain comes at an increase of the decoder memory from 1 to 5.

Fig. 4 presents the results of Proposition 2 on the link ergodic capacity for two different values of $N$. As expected, (25) and (26) become tight as $N_{\rm eff} \to \infty$ and $N_{\rm eff} \to 0$,

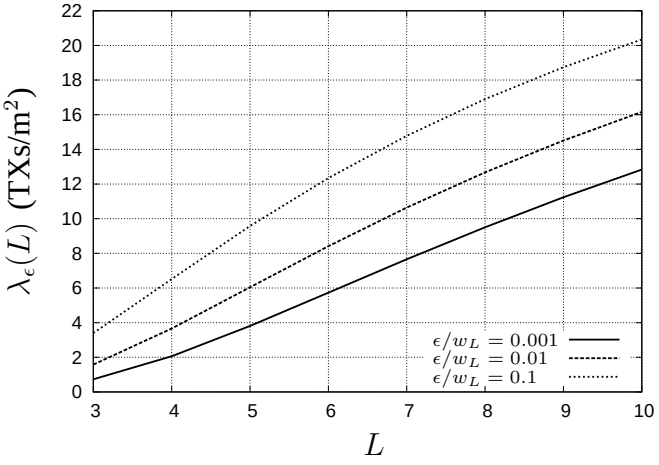


Fig. 3. Maximum contention density vs. $L$ for different values of $\epsilon/w_L$ ($R = 1$ m, QPSK, $L_{\rm b} = 800$, $N = 2$, $b = 4$, perfect CSI).

respectively. In Fig. 5, we employ the channel estimation scheme of Section V and examine the effect of imperfect CSI via simulation, when $L_{\rm b} = 500$, $D = 25$ and $T_d = 20$. As $T_p$ is increased the performance loss is reduced, at the expense of information rate, e.g., at $T_p = 10$, the rate-loss factor is $2/3$.

Finally, in Fig. 6, the simulated FEP of Enc2 and Enc4 are plotted vs. $N_{\rm eff}^{-1}$, for a channel with lognormal shadowing ($\sigma_s = 6$ dB) and shadowing-inversion PC or no PC. For small $N_{\rm eff}$, PC introduces a substantial gain, e.g., for Enc4 at $N_{\rm eff}^{-1} = 10$ dB, this gain is an order of magnitude. The reason for this is that the detrimental effect of shadowing to $\text{RX}_0$ is canceled and, at the same time, the interferer process is sparse enough such that the code protects $\text{RX}_0$ in the unlikely event of a large interfering power from a nearby interferer (this occurs when deep shadowing afflicts the channel between that interferer and its respective RX). Theoretically, we can see this with the help of Jensen's inequality: Given that all shadowing variables are i.i.d., by the definitions of $\delta_{\rm pc}$ and $\delta_{\rm npc}$ in Section V-D, we

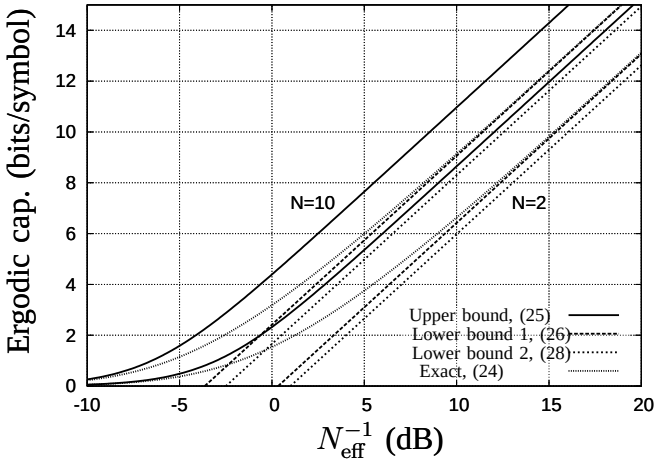


Fig. 4. Link ergodic capacity vs. $N_{\rm eff}^{-1}$. The two groups of curves correspond to $N = 2, 10$ ($b = 4$).

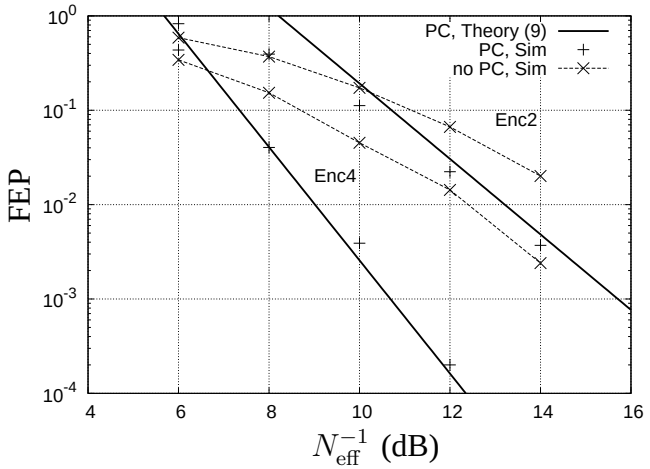


Fig. 6. FEP vs. $N_{\rm eff}^{-1}$ for Enc2 and Enc4 with/without PC (QPSK, $L_{\rm b} = 500$, $D = 25$, $T_d = 20$, $N = 2$, $b = 4$, perfect CSI, $\sigma_s = 6$).

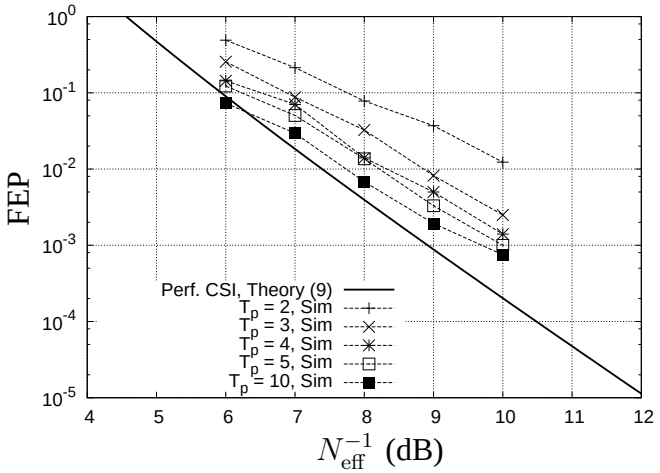


Fig. 5. FEP vs. $N_{\rm eff}^{-1}$ for Enc1 and different values of $T_p$. For $T_p = 5$ and a rate-loss factor of $20\%$ there is a 1 dB penalty compared to the perfect-CSI case (QPSK, $L_{\rm b} = 500$, $D = 25$, $T_d = 20$, $N = 2$, $b = 4$).

have that $\delta_{\rm pc}^l = \mathbb{E}[S^\alpha]^l \mathbb{E}[S^\alpha]^l < \mathbb{E}[S^{\alpha l}]\mathbb{E}[S^\alpha]^l = \delta_{\rm npc}^l$. Hence, from Proposition 1, PC should perform better in the small FEP regime, which is verified by Fig. 6. On the other hand, as the network becomes very dense, the diversity in the received signal is lost and the decoder is overwhelmed by an increased interference level due to PC. This is more apparent for Enc2 than Enc4, since Enc2 has a smaller Hamming distance. On a final note, we observe that, in the case of PC, there is good agreement between the theoretical FEP evaluated by (9) and the simulation results.

## VII. Concluding remarks

In this paper we considered FH during packet transmission and coding, as a physical-layer scheme for random wireless networks with uncoordinated transmissions. We demonstrated via analysis and simulation that the transmission capacity scales as $\epsilon^{1/L}$, where $\epsilon$ is the constraint placed on the packet error probability and $L$ is the code diversity order. A byproduct of our analysis was the derivation of a compact expression for the pdf of the SIR in a Rayleigh fading and $\alpha$-stable interference channel, when the RX performs MRC. Upper and lower bounds on the ergodic capacity of this channel were also derived.

Employing a simple channel estimation algorithm based on the transmission of pilot symbols at the beginning of each dwell, we showed that the performance degradation due to imperfect CSI is reasonable, at a rate loss of the order of $20\%$. The effect of channel-inversion PC was also investigated for a channel with lognormal shadowing, and PC was shown to be beneficial if $\lambda/M$ is sufficiently small. In conclusion, we believe that, given the gains in terms of network capacity at moderate encoding/decoding complexity, even for a small number of subbands, this scheme merits consideration despite the increased overhead compared to a slow FH system.

## References


[1] M. Haenggi, J. G. Andrews, F. Baccelli, O. Dousse, and M. Franceschetti, "Stochastic geometry and random graphs for the analysis and design of wireless networks," *IEEE J. Sel. Areas Commun.*, vol. 27, pp. 1029–1046, Sep. 2009.

[2] S. P. Weber, J. G. Andrews, and N. Jindal, "The effect of fading, channel inversion and threshold scheduling on ad hoc networks," *IEEE Trans. Inf. Theory*, vol. 53, pp. 4127–4149, Nov. 2007.

[3] D. N. C. Tse and P. Viswanath, *Fundamentals of Wireless Communication*, 1st ed. Cambridge University Press, 2005.

[4] K. Stamatiou, J. G. Proakis, and J. R. Zeidler, "Evaluation of MIMO techniques in FH-MA ad hoc networks," in *Proc. IEEE GLOBECOM*, Washington D.C., Nov. 2007.

[5] G. Caire, G. Taricco, and E. Biglieri, "Bit-interleaved coded modulation," *IEEE Trans. Inf. Theory*, vol. 44, pp. 927–946, May 1998.

[6] J. G. Andrews, S. Weber, and M. Haenggi, "Ad hoc networks: to spread or not to spread?" *IEEE Commun. Mag.*, pp. 84–91, Dec. 2007.

[7] E. Geraniotis and J. W. Gluck, "Coded FH/SS communications in the presence of combined partial-band noise jamming, rician nonselective fading and multiuser interference," *IEEE J. Sel. Areas Commun.*, vol. 5, pp. 194–214, Feb. 1987.

[8] C. W. Baum and M. B. Pursley, "Erasure intertion in FH communications with fading and partial-band interference," *IEEE Trans. Veh. Technol.*, vol. 46, pp. 949–956, Nov. 1997.

[9] J. G. Proakis and M. Salehi, *Digital Communications*, 5th ed. Mc Graw Hill, 2008.

[10] M. W. Subbarao and B. L. Hughes, "Optimal transmission ranges and code rates for frequency-hop packet radio networks," *IEEE Trans. Commun.*, vol. 4, pp. 670–678, Apr. 2000.

[11] H. Sui and J. R. Zeidler, "Information efficiency and transmission range optimization for coded MIMO FH-CDMA networks in time-varying environments," *IEEE Trans. Commun.*, vol. 57, pp. 481–491, Feb. 2009.

[12] E. S. Sousa and J. A. Silvester, "Optimum transmission ranges in a direct-sequence spread-spectrum multi-hop packet radio network," *IEEE J. Sel. Areas Commun.*, vol. 8, pp. 762–771, Jun. 1990.
[13] G. Caire and E. Viterbo, "Upper bound on the frame error probability of terminated trellis codes," *IEEE Commun. Lett.*, vol. 2, pp. 2–4, Jan. 1998.
[14] F. Baccelli, B. Błaszczyszyn, and P. Mühlethaler, "An Aloha protocol for multi-hop mobile wireless networks," *IEEE Trans. Inf. Theory*, vol. 52, pp. 421–436, Feb. 2006.
[15] M. K. Simon and D. Divsalar, "Some new twists to problems involving the Gaussian probability integral," *IEEE Trans. Commun.*, vol. 46, pp. 200–210, Feb. 1998.
[16] I. S. Gradshteyn and I. M. Ryzhik, *Table of integrals, series and products*, 4th ed. Academic Press, 1994.
[17] A. M. Hunter, J. G. Andrews, and S. P. Weber, "Capacity scaling of ad hoc networks with spatial diversity," *IEEE Trans. Wireless Commun.*, vol. 7, pp. 5058–5071, Dec. 2008.
[18] D. W. B. S. Govindasamy and D. H. Staelin, "Spectral efficiency in single-hop ad hoc wireless networks with interference using adaptive antenna arrays," *IEEE J. Sel. Areas Commun.*, vol. 25, pp. 1358–1369, Sep. 2007.
[19] R. M. Young, "Euler's constant," *The Mathematical Gazette*, vol. 75, pp. 187–190, 1991.
[20] S. M. Kay, *Fundamentals of statistical signal processing: estimation theory*, 1st ed. Prentice Hall, 1993.
[21] R. K. Ganti and M. Haenggi, "Spatial and temporal correlation of the interference in Aloha ad hoc networks," *IEEE Commun. Lett.*, vol. 13, pp. 631–633, Sep. 2009.
[22] M. L. Cedervall and R. Johannesson, "A fast algorithm for computing distance spectrum of convolutional codes," *IEEE Trans. Inf. Theory*, vol. 35, pp. 1146–1159, Nov. 1989.

**Kostas Stamatiou** Kostas Stamatiou received his Diploma in Electrical and Computer Engineering from the National Technical University of Athens in 2000, and the M.Sc. and Ph.D. in Electrical Engineering from the University of California San Diego in 2004 and 2009, respectively. He is currently a post-doctoral scholar in the Department of Electrical Engineering at the University of Notre Dame.

His general research interests lie in the areas of error correction coding, frequency-hopping systems and ad hoc networks. He is currently working on the application of stochastic geometric techniques in the analysis and design of large wireless networks.

**John G. Proakis** John G. Proakis (S'58-M'62-F'84-LF'99) received the BSEE from the University of Cincinnati in 1959, the MSEE from MIT in 1961 and the Ph.D. from Harvard University in 1967. He is an Adjunct Professor at the University of California at San Diego and a Professor Emeritus at Northeastern University. He was a faculty member at Northeastern University from 1969 through 1998 and held the following academic positions: Associate Professor of Electrical Engineering, 1969-1976; Professor of Electrical Engineering, 1976-1998; Associate Dean of the College of Engineering and Director of the Graduate School of Engineering, 1982-1984; Interim Dean of the College of Engineering, 1992-1993; Chairman of the Department of Electrical and Computer Engineering, 1984-1997. Prior to joining Northeastern University, he worked at GTE Laboratories and the MIT Lincoln Laboratory.

His professional experience and interests are in the general areas of digital communications and digital signal processing. He is the co-author of the following books: Digital Communications (New York: McGraw-Hill, 2008, fifth edition), Introduction to Digital Signal Processing (Upper Saddle River: Prentice Hall, 2007, fourth edition); Digital Signal Processing Laboratory (Englewood Cliffs: Prentice Hall, 1991); Advanced Digital Signal Processing (New York: Macmillan, 1992); Algorithms for Statistical Signal Processing(Upper Saddle River: Prentice Hall, 2002); Discrete-Time Processing of Speech Signals (New York: Macmillan, 1992, IEEE Press, 2000); Communication Systems Engineering, (Upper Saddle River: Prentice Hall, 2002, second edition); Digital Signal Processing Using MATLAB V.4 (Boston: Brooks/Cole-Thomson Learning, 2007, second edition); Contemporary Communication Systems Using MATLAB (Boston: Brooks/Cole-Thomson Learning, 2004, second edition); Fundamentals of Communication Systems (Upper Saddle River: Prentice Hall, 2005).

**James R. Zeidler** Dr. James Zeidler is a research scientist/senior lecturer in the Department of Electrical Engineering at the University of California, San Diego. He is a faculty member of the UCSD Center for Wireless Communications and the University of California Institute for Telecommunications and Information Technology. He has more than 200 technical publications and fourteen patents for communication, signal processing, data compression techniques, and electronic devices. Dr. Zeidler was elected Fellow of the IEEE in 1994 for his technical contributions to adaptive signal processing and its applications. He was co-author of the best student paper at the 2006 IEEE Personal, Indoor, and Mobile Radio Conference, received the Frederick Ellersick best paper award from the IEEE Communications Society at the IEEE Military Communications Conference in 1995, the Navy Meritorious Civilian Service Award in 1991, and the Lauritsen-Bennett Award for Achievement in Science from the Space and Naval Warfare Systems Center in 2000. He was an Associate Editor of the IEEE Transactions on Signal Processing.